

Communication

# Survivin-Sodium Iodide Symporter Reporter as a Non-Invasive Diagnostic Marker to Differentiate Uterine Leiomyosarcoma from Leiomyoma

Natalia Garcia <sup>1,2,†</sup>, Mara Ulin <sup>1,3,†</sup>, Qiwei Yang <sup>1,4</sup> , Mohamed Ali <sup>1,4,5</sup> , Maarten C. Bosland <sup>6</sup>, Weiqiao Zeng <sup>1</sup>, Liaohai Chen <sup>1</sup> and Ayman Al-Hendy <sup>1,4,\*</sup> 

- <sup>1</sup> Department of Surgery, University of Illinois at Chicago, Chicago, IL 60607, USA; natalia.garciaft@gmail.com (N.G.); maraulin1989@hotmail.com (M.U.); yangq@bsd.uchicago.edu (Q.Y.); mohamed.ali@bsd.uchicago.edu (M.A.); wzeng9@uic.edu (W.Z.); lhchen@uic.edu (L.C.)
- <sup>2</sup> Greehey Children's Cancer Research Institute, The University of Texas Health Science Center, San Antonio, TX 77030, USA
- <sup>3</sup> Department of Obstetrics and Gynecology, Mount Sinai Hospital, Chicago, IL 11537, USA
- <sup>4</sup> Department of Obstetrics and Gynecology, University of Chicago, Chicago, IL 60637, USA
- <sup>5</sup> Clinical Pharmacy Department, Faculty of Pharmacy, Ain Shams University, Cairo 11566, Egypt
- <sup>6</sup> Department of Pathology, University of Illinois at Chicago, Chicago, IL 60607, USA; boslandm@uic.edu
- \* Correspondence: aalhendy@bsd.uchicago.edu
- † These authors contributed equally to this work.

**Abstract:** Leiomyosarcoma (LMS) has been challenging to diagnose because of limitations in clinical and radiographic predictors, as well as the lack of reliable serum or urinary biomarkers. Most uterine masses consist of benign leiomyoma (LM). However, it is currently a significant challenge in gynecology practice to differentiate LMS from LM. This inability poses grave consequences for patients, leading to a high number of unnecessary hysterectomies, infertility, and other major morbidities and possible mortalities. This study aimed to evaluate the use of Survivin-Sodium iodide symporter (Ad-Sur-NIS) as a reporter gene biomarker to differentiate malignant LMS from benign LM by using an F18-NaBF<sub>4</sub> PET/CT scan. The PET/CT scan images showed a significantly increased radiotracer uptake and a decreased radiotracer decay attributable to the higher abundance of Ad-Sur-NIS in the LMS tumors compared to LM ( $p < 0.05$ ). An excellent safety profile was observed, with no pathological or metabolic differences detected in Ad-Sur-NIS-treated animal versus the vehicle control. Ad-Sur-NIS as a PET scan reporter is a promising imaging biomarker that can differentiate uterine LMS from LM using F18-NaBF<sub>4</sub> as a radiotracer. As a new diagnostic method, the F18 NaBF<sub>4</sub> PET/CT scan can provide a much-needed tool in clinical practices to effectively triage women with suspicious uterine masses and avoid unnecessary invasive interventions.

**Keywords:** uterine mass; uterine leiomyosarcoma; uterine leiomyoma; PET/CT scan



**Citation:** Garcia, N.; Ulin, M.; Yang, Q.; Ali, M.; Bosland, M.C.; Zeng, W.; Chen, L.; Al-Hendy, A. Survivin-Sodium Iodide Symporter Reporter as a Non-Invasive Diagnostic Marker to Differentiate Uterine Leiomyosarcoma from Leiomyoma. *Cells* **2023**, *12*, 2830. <https://doi.org/10.3390/cells12242830>

Academic Editors: Alessandro Grinzato, Vittoria Raimondi and J. Bernard Heymann

Received: 23 October 2023  
Revised: 4 December 2023  
Accepted: 8 December 2023  
Published: 13 December 2023



**Copyright:** © 2023 by the authors. Licensee MDPI, Basel, Switzerland. This article is an open access article distributed under the terms and conditions of the Creative Commons Attribution (CC BY) license (<https://creativecommons.org/licenses/by/4.0/>).

## 1. Introduction

Annually, around twenty-six million patients present with uterine masses [1–3]. Uterine leiomyoma (LM) is the most common benign female pelvic neoplasm [4,5]. By age 50, around 80% of African Americans and 70% of Caucasian women will have LM [6]. Uterine leiomyosarcoma (uLMS) is a highly aggressive gynecology malignant mesenchymal tumor of myometrial smooth-muscle derivation. It is the most common type of uterine sarcoma, with low survival rates, representing 60% and accounting for approximately 1–2% of uterine malignancies [7–10]. uLMS is less common than LMs and has a worse prognosis [11].

Both LM and LMS manifest as focal masses in the uterus that can be accompanied by abnormal uterine bleeding, pelvic pressure, and/or pain. The clinical evaluation of a pelvic mass includes a complete medical history and an abdominal and pelvic examination. Sadly, there is frequently no discernible difference between the clinical characteristics of

uterine sarcomas and benign LM. A pelvic ultrasound is typically ordered as the first imaging test for patients with a pelvic tumor. Imaging studies frequently lack the ability to demonstrate any difference between LMs and uterine sarcomas, which are both localized tumors inside the uterus that may have central necrosis. Despite these drawbacks, this is part of the first-line workup. Endometrial sampling is frequently performed in patients with abnormal uterine bleeding and pelvic mass to identify neoplasia. Still, only 33 to 68 percent of individuals with uterine sarcomas receive a diagnosis of sarcoma from an endometrial biopsy.

Treatment options for LM include expectant, medical, interventional, and surgical therapies. Treatment objectives should be specified for each patient, taking into account the primary symptomatology, such as bleeding and bulk symptoms, as well as the desire to preserve the uterus and future fertility [12]. Evaluation includes risk stratification and the use of imaging, cervical cancer screening and endometrial tissue sampling to identify malignancy [13].

When surgical treatment is desired, treatment options include myomectomy and hysterectomy. Whenever possible, the least invasive route is advised. Minimal invasive surgery, either laparoscopic or robotic surgery, compared to laparotomy, is associated with less postoperative pain, shorter hospitalization, a lower risk of postoperative fever, and a faster return to work [13]. When utilizing the least invasive procedure, uterine morcellation is occasionally used to retrieve the uterus or LM. Nevertheless, it is important to be aware of the cancer risk because women who undergo minimally invasive surgery and have undiagnosed uLMS may be more likely to experience an increase in morbidity due to the spread of cancer cells during the procedure [14,15].

The true prevalence of uLMS is unknown [16,17]. Based on the 2017 agency for healthcare research and quality report, which used the largest dataset to determine the estimate of the prevalence of uLMS, the risk of unexpected uLMS in surgeries performed for symptomatic LM can range from 1 in 770 surgeries to less than 1 in 10,000 surgeries [18]. In addition, diagnostic biomarkers to distinguish benign LM versus malignant LMS have not been established yet. Although the levels of serum CA125 and LDH were elevated in uLMS, the sensitivity and specificity were low [19]. Currently, no diagnostic tool (laboratory test or imaging study) can provide a differential diagnosis between LM and uLMS before surgical intervention [7,20,21]. LM and LMS tumors present with similar symptoms (abnormal uterine bleeding, pelvic mass, and pelvic pain). By contrast, the clinical outcome for these tumors is entirely different [22].

A major challenge for gynecologists is to differentiate LM from LMS before surgery. At present, there are no pathognomonic signs, symptoms, reliable radiographic predictors, or biomarkers (serum or urinary markers) to differentiate between these two conditions [7,20,21,23–25].

The FDA has recommended limiting the use of laparoscopic power morcellation in women with suspected or confirmed cancer undergoing gynecological surgeries. Diagnosing uLMS before surgery can be crucial for an improved patient outcome, by providing a better treatment approach. The LM patient can benefit from an early differential diagnosis to avoid unnecessary surgeries, or can choose non-invasive surgery. In contrast, the uLMS patient can have a timely intervention for this aggressive disease.

This study aimed to evaluate the efficacy and safety of Survivin-Sodium iodide symporter (Ad-Sur-NIS) as a reporter gene biomarker to differentiate between uterine LM from uLMS by positron emission tomography (PET) imaging using LM and LMS xenograft mouse models (Figure 1).

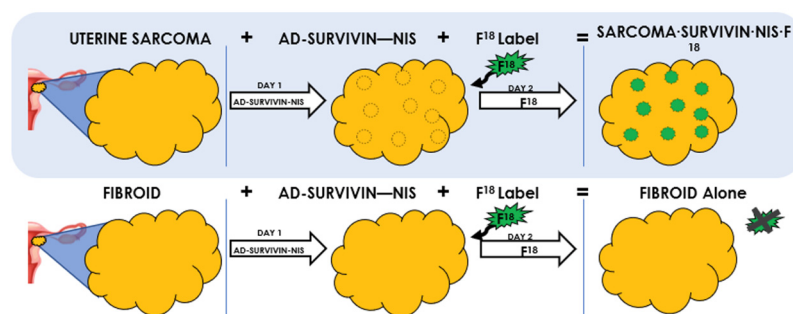


**Figure 1.** Adenovirus Survivin-Sodium Iodide Symporter (Ad-Sur-NIS) System. It is a gene-based bioimaging tool to differentiate between LM and LMS in women with suspicious uterine masses. Uterine LMS and LM cannot be differentiated using current imaging techniques. Survivin is increased in LMS, but not in LM. Using Ad-SUR-NIS, we were able to detect NIS in the presence of Survivin. NIS enables the uptake of F18- $\text{NaBF}_4$  to cells, which leads to the visualization and identification of uterine LMS, but not LM.

## 2. Materials and Methods

### 2.1. Human Leiomyoma and Human Uterine Leiomyosarcoma Cells

Immortalized human LM cells were cultured in phenol red-free 10% fetal bovine serum Dulbecco's Modified Eagle Medium: Nutrient Mixture F-12. Human LMS cells (SK-UT1, ATCC<sup>®</sup> HTB-114<sup>™</sup>) (ATCC, Manassas, VA, USA) were cultured in ATCC-formulated Eagle's Minimum Essential Medium with 10% fetal bovine serum.

### 2.2. Reagents

The Ad-Sur-NIS was produced by Vector Biolabs (Malvern, PA, USA). The PET imaging tracer, F18-labeled sodium tetrafluoroborate (F18- $\text{NaBF}_4$ ), was purchased from the Cyclotron Facility at the University of Chicago (Chicago, IL, USA).

### 2.3. Animal Model

The mice were handled according to the IACUC-approved protocol (18-174). Fifty-four nu/nu nude mice were purchased from Charles River. The mice were provided with autoclaved water and a standard natural ingredient diet ad libitum and were maintained in an AAALAC-accredited pathogen-free climate-controlled facility at a 12 h light/dark cycle;  $2 \times 10^7$  LMS or LM cells were inoculated into the right flank in 1:1 Matrigel and fetal bovine serum (FBS). After tumor development, the animals were randomized and separated into groups: LMS Ad-Sur-NIS, LMS PBS, LM Ad-Sur-NIS, and LM PBS. PBS was used as a vehicle for Ad-Sur-NIS administration.

### 2.4. PET/CT Scan

A total of 40 animals (LMS Ad-Sur-NIS  $n = 10$ , LMS PBS  $n = 10$ , LM Ad-Sur-NIS  $n = 10$ , and LM PBS  $n = 10$ ) were imaged with PET/CT using a micro-PET/CT scanner (Trans-PET Discoverist 80, Raycan Technology Co., Ltd., Suzhou, China). Twenty-four hours before the PET/CT imaging, the animals received a dose of either Ad-Sur-NIS ( $1 \times 10^9$  PFU in 0.2 mL/mouse) or PBS (0.2 mL/mouse) through retro-orbital injection. On the day of the PET/CT scan, a dose of 300–400  $\mu\text{Ci}$  of F18- $\text{NaBF}_4$  was given intravenously through a tail-vein injection under isoflurane anesthesia. The anesthesia was continued, and the mice were placed on the sample stage of the PET scanner on a heating pad. Two PET/CT scans were conducted for each mouse, the first immediately, 5 min after injection of F18- $\text{NaBF}_4$ , and the second scan was run after 45 min (Figure 2). Each scan lasted 10 min in static mode, and the mice were taken out of the PET/CT scan machine between the two scans. The PET and CT images were reconstructed using PiSYS software (version 1.3, Raycan Technology Co., Ltd.) associated with the scanner and were exported in DICOM format for analysis.

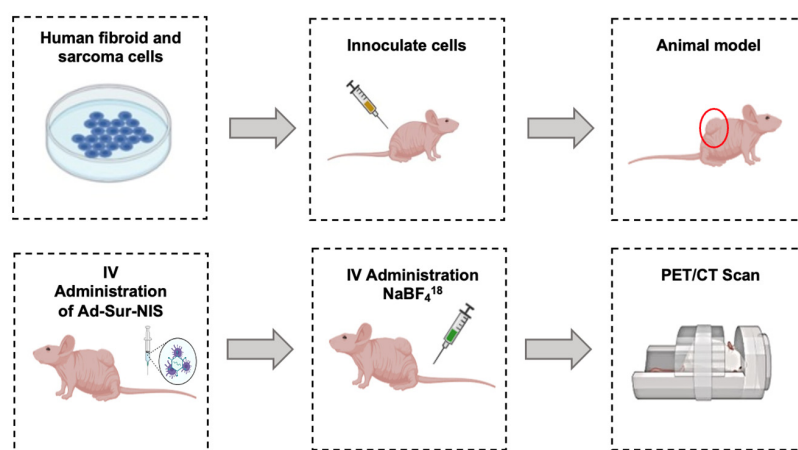


**Figure 2.** Experimental Design. uLMS and uterine LM cells were cultivated. The cells were inoculated in the right flank of the nude mice. After tumor development, the animals received an intravenous administration of Ad-Sur-NIS or PBS. Then, 24 h later, all the animals received F18-NaBF<sub>4</sub> through intravenous administration, and PET/CT scans were performed.

### 2.5. PET/CT Scan Analysis

Carimas 2.10 (Turku PET Centre, Turku, Finland) was used to analyze the PET images. A 3-dimensional region of interest (ROI) was drawn for the tumor area in each mouse. Corresponding CT images were overlaid with the PET images as an anatomical reference. The ROI was smoothed once before the PET intensities (i.e., the F18 activities) were exported. The standardized uptake value (SUV<sub>max</sub> or SUV<sub>mean</sub>) for each ROI was calculated by using the formula  $SUV = \frac{A/\rho}{D/W}$ , where A is the maximum or mean F18-NaBF<sub>4</sub> activity of the ROI,  $\rho$  is the density of the mouse (~1 g/mL), D is the total injected dose, and W is the weight of the mouse. SUV<sub>max</sub> values were used to create the graphics.

### 2.6. Safety Study—H&E Stain and Chemical Metabolic Panel

Fourteen animals were used to determine the safety of Ad-Sur-NIS (LMS Ad-Sur-NIS n = 4, LMS PBS n = 4, LM Ad-Sur-NIS n = 3, LM PBS n = 3). Twenty-four hours after the Ad-Sur-NIS injection, blood (serum) and organ (brain, kidney, liver, lung, heart, ovary, uterus spleen, and tumor) samples were collected. Serum samples were used to evaluate the liver function and a blood chemistry panel was performed by the Biological Laboratories Resource Laboratory Services unit. Organ samples were fixed in 10% buffered formalin for 24 h, then processed and embedded in paraffin, and 5-micron sections were made and stained with H&E. The H&E slides were evaluated by a veterinary pathologist (MCB).

### 2.7. Statistical Analysis

Data were presented as mean  $\pm$  standard error (SE). A significant difference was defined as  $p < 0.05$ . A comparison of the 2 groups was carried out using the parametric Student's *t*-test for normally distributed data and a nonparametric Mann–Whitney test for not-normally distributed data. A comparison of multiple groups was carried out by analysis of variance (ANOVA) followed by a Tukey post hoc test for normally distributed data parametric distribution and a Kruskal–Wallis test followed by Dunn's post hoc test for nonparametric not normally distributed data. The statistical analysis was carried out using GraphPad Prism 5 Software.

## 3. Results

### 3.1. Increased Radiotracer Uptake and Decreased Radiotracer Decay Attributable to Ad-Sur-NIS in the LMS Tumors When Compared to LM

The Ad-Sur-NIS was constructed based on our previous results [26], showing that ad-Sur-Luc could differentiate LMS from LM. We selected the NIS to be used as a reporter gene, and its expression can be detected through a PET scan using F18-NaBF<sub>4</sub> as a radiotracer, allowing Ad-Sur-NIS to be used as a human application in the future.

After the mice PET/CT scanning, we identified no uptake difference among the groups at the early capture time point (5 min after radiotracer administration). However, at the late capture (at minutes 45 after administration), we were able to differentiate uLMS tumors from LM tumors using Ad-Sur-NIS ( $p < 0.05$ ), as demonstrated in Figure 3A,B. Along with these findings, we also found that the use of Ad-Sur-NIS decreased radiotracer decay (comparing early and late capture) in LMS tumors compared to LM tumors ( $p < 0.05$ ), allowing us to further differentiate one condition from the other (Figures 3B and 4).

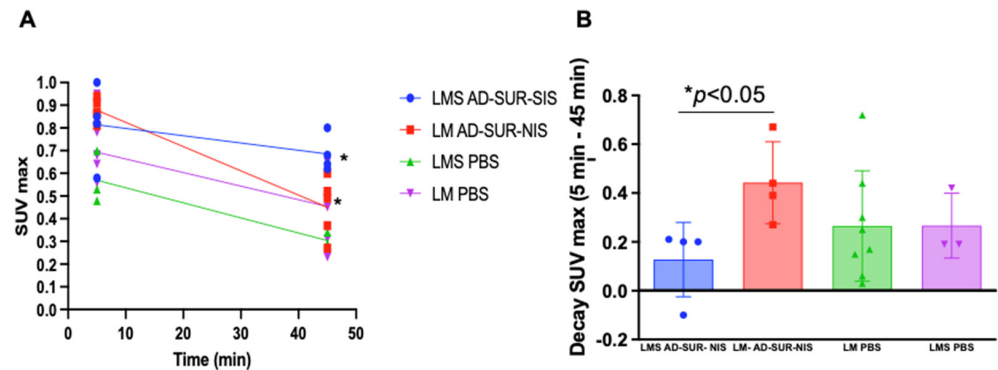


**Figure 3.** Increased uptake of the F18-labeled tracer attributable to Ad-Sur-NIS in uLMS. (A) PET/CT scan identifies uptake time after 5 and 45 min radiotracer administration. At minute 45, a significant difference between LMS Ad-Sur-NIS versus LM Ad-Sur-NIS was  $p < 0.05$ . (B) Decrease in SUV max decay between minutes 5 and 45 in LMS Ad-Sur-NIS compared to LM Ad-Sur-NIS  $p < 0.05$ .

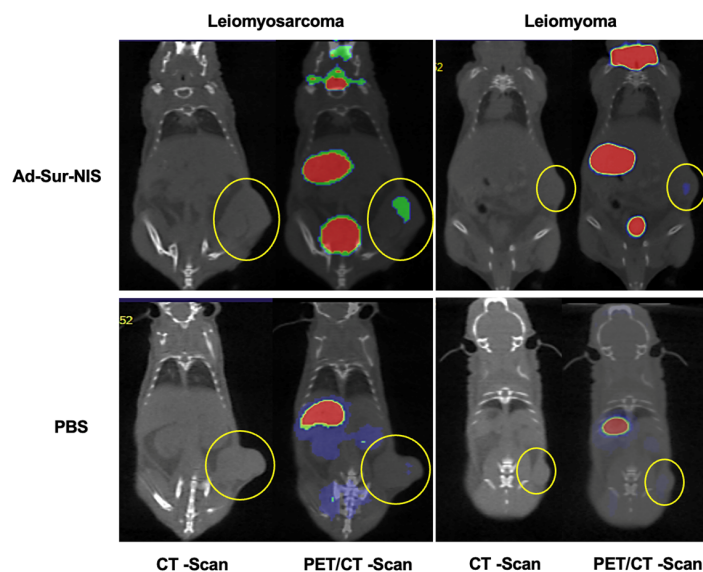


**Figure 4.** PET/CT images of Ad-Sur-NIS treated mice and control mice (treated with PBS). The PET/CT scans were performed 45 minutes after the F18-NaBF<sub>4</sub> administration. The tumors are identified in CT images as indicated by the yellow circles. The uptake intensities of F18-NaBF<sub>4</sub> are “rainbow” color-coded from red (high intensity) to green (medium intensity) to blue (low intensity). While large amounts of F18-NaBF<sub>4</sub> are presented in the bladder, stomach, and thyroid as intrinsic uptake/distribution, the uptake of F18-NaBF<sub>4</sub> in LMS is clearly visualized (green color), while the uptake of F18-NaBF<sub>4</sub> in LM is minimal. Control experiments with mice treated with PBS (instead of Ad-Sur-NIS) indicated no uptake of F18-NaBF<sub>4</sub> in both LMS and LM. The results indicated that the F18-NaBF<sub>4</sub> PET/CT scan is capable of differentiating malignant LMS from benign LM.

### 3.2. Evaluation of the Safety of Ad-Sur-NIS

Our study revealed that the administration of Ad-Sur-NIS did not cause differences in a metabolic chemistry panel compared to the PBS group (Table 1). Specifically, we did not find evidence of drug-induced liver injury (Table 2).

We did not observe evidence of tissue injury or morphologic differences between the Ad-Sur-NIS and PBS groups in the brain, heart, kidney, liver, lung, ovary, spleen, and uterus (Figure 5).

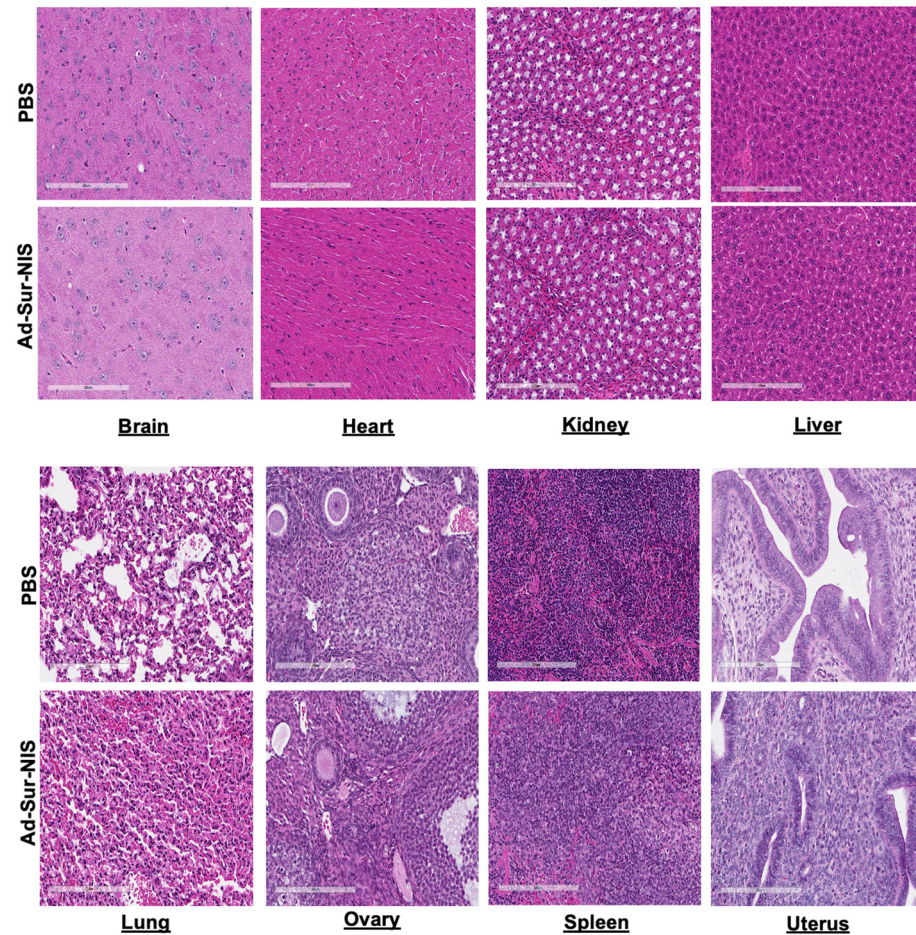


**Figure 5.** Histologic evaluation of Ad-Sur-NIS. After 24 h of the Ad-Sur-NIS or PBS injection, the various organs, including brain, kidney, liver, lung, heart, ovary, uterus, and spleen, were collected and H&E stain was performed.

**Table 1.** The chemistry metabolic panel evaluated after the administration of Ad-Sur-NIS or vehicle (PBS).

Parameter	LMS AD-SUR-NIS	LM AD-SUR-NIS	LMS PBS	LM PBS	<i>p</i> -Value
Albumin g/dL	3.002 (±0.12)	2.93 (±0.11)	3.41 (±0.15) *	2.88 (±0.075) *	0.025
Alkaline Phosphatase (ALP) U/L	102.25 (±37.31)	102.33 (±21.54)	91.5 (±4.50)	90.33 (±5.85)	0.94
Alanine Aminotransferase (ALT) U/L	34.5 (±8.38)	51.33 (±23.28)	30.5 (±7.35)	35.66 (±12.01)	0.346
Amylase U/L	422.25 (±52.94)	411.66 (±46.09)	416.25 (±63.17)	402.33 (±32.53)	0.0814
Aspartate Aminotransferase (AST) U/L	259.75 (±84.98)	367.33 (±159.2022)	253 (±178.095)	256.66 (±144.68)	0.8157
Urine Nitrogen (BUN) mg/dL	20.25 (±5.29)	25.66 (±2.08)	23.5 (±3.31)	28 (±2.64)	0.3171
Creatinine Kinase U/L	2994.75 (±2379.35)	3251.33 (±1632.798)	1782.75 (±1897.929)	2337.5 (±1546.443)	0.59
Creatinine mg/dL	0.0686 (±0.3538)	0.0153 (±0.124)	0.0724 (±0.0945)	0.0665 (±0.0156)	0.606
Direct Bilirubin mg/dL	0.0275 (±0.015)	0.0166 (±0.0115)	0.03 (±0.008)	0.0266 (±0.0115)	0.47
Gamma Glutamyl Transferase (GGT) U/L	−6.25 (±4.34)	−8.33 (±5.68)	−7 (±3.829)	−6.33 (±5.131)	0.93
Lactate mg/dL	67.95 (±10.51)	57.866 (±8.87) *	93.425 (±12.28) *	41.9 (±3.49)	0.0357
I Phosphorus mg/dL	7.57 (±1.36)	7.13 (±0.64) *	13.45 (±0.50) *	9 (±1.70)	0.0274
Total Bilirubin md/dL	0.3025 (±0.124)	0.29 (±0.167)	0.375 (±0.118)	0.32 (±0.075)	0.7576
Total Protein g/dL	4.795 (±0.21)	4.67 (±0.2497)	5.312 (±0.217) *	4.48 (±0.169) *	0.0206
Globulin g/dL	1.791 (±0.101)	1.738 (±0.137)	1.893 (±0.081) *	1.6088 (±0.074) *	0.047
Alb/ Glob Ratio	2 (±0)	2 (±0)	2 (±0)	2 (±0)	1

\* = *p* < 0.05.

**Table 2.** Calculation of the ratio of ALT and ALP to assess the type of drug-induced liver injury.

Ratio of ALT and ALP	LMS-AD-SUR-NIS	LM-AD-SUR-NIS	LMS PBS	LM PBS
	0.419	0.623	0.414	0.490

ALT = alanine aminotransferase; ALP = alkaline phosphatase; R = ratio; ULN = upper limit of normal. Interpretation:  $\geq 5$  in hepatocellular injury,  $< 2$  in cholestatic liver injury, between 2 and 5 in mixed hepatocellular/cholestatic liver injury.

#### 4. Discussion

In this study, Ad-Sur-NIS *in vivo* showed that the Survivin promoter could drive NIS expression, specifically in malignant uLMS cells. This is consistent with our previous study showing that human uLMS cells highly expressed the luciferase reporter gene driven by the Survivin promoter compared to benign LM [18]. However, a new probe with a clinical application was needed due to limitations in the use of luciferase as a reporter gene for human application. The human sodium/iodide symporter (NIS), an intrinsic membrane glycoprotein with 13 putative transmembrane domains, plays an essential role in the biosynthesis of thyroid hormones by mediating the active transport of iodide into the thyrocytes [27].

The tumor-specific expression of NIS genes has been identified in many types of tumors, including prostate, colon, and liver cancer, suggesting that NIS expression under the control of tissue-specific promoters could be helpful in diagnostic and therapeutic applications [27–30]. Notably, adenosine triphosphatase copper ion transporting beta expression is aberrantly upregulated in uLMS cells, and copper sulfate acts as an inhibitor of platinum efflux via the transporter. Combining copper sulfate pretreatment with cisplatin administration exhibited an antitumor effect in mice with uLMS cell xenografts [31]. Using the relevant knowledge, we were able to use Ad-Sur-NIS to distinguish LMS from LM xenografts in nude mice using PET/CT scanning by comparing radiotracer uptake and decay, which may offer a promising non-invasive diagnostic tool to determine malignant LMS from benign LM.

uLMS is a rare and highly aggressive tumor with a 5-year survival of 10–15% for women with metastatic disease. By contrast, LM is benign and common, with up to 70–80% of women developing LM during their lifetime. The differential diagnosis between these two tumors is challenging since the clinical symptoms of both tumors overlap, and more than 50% of women with LMS are initially treated as having LM with potentially inadequate or non-oncology surgery, risking worse outcomes [32]. Although malignant uLMS and benign LM share some common clinical characteristics [33], the molecular signature and biological pathways differ between these two kinds of tumors [34–38]. To overcome the limitations in clinical and radiographic predictors, as well as the lack of reliable serum or urinary biomarkers, the development of a new clinical tool to differentiate LMS from LM in gynecologic practice is urgently needed to select the correct treatment pathway for patients with a uterine mass.

There are several studies evaluating different tools to differentiate LM from LMS. However, the results are debatable, and no evidence is presented that any of these approaches could reliably distinguish LMS from LM [32,39–41]. Several imaging modalities, such as MRI, Doppler sonography, and positron emission tomography, have been attempted, but their predictive value still needs to be determined [41–43]. Ultrasonography is a standard imaging modality used in the gynecology clinic, but the similar appearances of LMS and LM limit its use for their differential diagnosis [32,44]. Although recent studies have demonstrated that MRI features could help differentiate LMS from LM, its use in LMS diagnosis is challenging because the appearance of LMS in MR images is variable and overlaps with features of degenerated LM [32,45].

The application of PET scans in oncology plays an important role in assessing early diagnosis and pharmacokinetics and pharmacodynamics of novel therapeutics using radio-labeled compounds [46]. As a non-invasive imaging methodology, PET has been utilized with the administration of compounds labeled with radiotracers that are formulated for intravenous injection. Several radionuclides for PET imaging have been used [47].

In this study, we used F18-NaBF<sub>4</sub> as a nuclide because it has a relatively long half-life, allowing for transport from the production site to the PET centers, high labeling yields, high specific activity, and a high resolution of images [48]. Moreover, the PET radioligand F18-NaBF<sub>4</sub> was used to image NIS. F18-NaBF<sub>4</sub> has been shown to increase uptake in known areas with high NIS expression without adverse effects [49]. In contrast to previously used iodides, F18-NaBF<sub>4</sub> and other F18-labeled iodide analogs have practical radiosynthesis and biochemical properties that allow them to mimic iodide transport by NIS closely [47].

In addition to imaging the LMS and LM, we also examined whether the administration of Ad-Sur-NIS caused any side effects or toxicity. We did not observe any pathological or metabolic changes or indications of liver injury. These studies indicate that Ad-Sur-NIS with the use of F18-NaBF<sub>4</sub> is safe in our experimental system and suggest that it may be considered a safe, non-invasive diagnostic tool in human application. Moreover, in combination with radioiodine therapy, this strategy has excellent potential for LMS gene therapy.

Notably, the expression of Survivin is detected in human cancers, but not in normal adult tissues. In this study, we used the cancer-specific enhanced Survivin promoter to determine the promoter driving potential of downstream reporter genes. We demonstrate that the F18 NaBF<sub>4</sub> PET/CT approach can distinguish benign LM from malignant uLMS. According to the “cancer-specific promoters’ hypothesis”, this new approach would provide useful information to triage suspicious lesions in order to distinguish benign tumors from uLMS and other gynecological cancers preoperatively. A potential issue is that using the Ad-Sur-NIS system in uLMS requires phase I assessment. However, similar studies have been reported in nuclear medicine, such as a thyroid scan for the evaluation of suspicious thyroid masses. Therefore, this approach has great potential to be adopted in clinical practice in the future.

## 5. Conclusions

In conclusion, the F18-NaBF<sub>4</sub> PET/CT scan using Ad-Sur-NIS is a promising and non-invasion diagnostic tool to distinguish malignant uLMS from benign counterparts. It has great potential to impact the management of suspicious uterine masses, a significant challenge in clinical gynecology.

## 6. Patents

The results from this manuscript are part of the US2021/0244832A1 patent.

**Author Contributions:** N.G. and M.U. were equally involved in the experimental design, performing of experiments, data analysis, and the writing of the manuscript. Q.Y.: writing manuscript and manuscript revision. M.A.: Involved in the experimental work of the study. M.C.B.: Performed histopathologic analysis and manuscript revision. W.Z. and L.C.: designed, performed, analyzed, and presented the PET/CT experiments and results. A.A.-H.: Conceptual design and manuscript revision. All authors have read and agreed to the published version of the manuscript.

**Funding:** This work was supported by the University of Illinois at Chicago—Proof of concept 2020; National Institutes of Health (NIH) (grants RO1 HD094378; RO1 ES028615; U54 MD007602, RO1 HD094380 and RO1 HD106285).

**Institutional Review Board Statement:** All applicable international, national, and/or institutional guidelines for the care and use of animals were followed, and IACUC (18-174) approval of University of Illinois at Chicago was given.

**Informed Consent Statement:** Not applicable.

**Data Availability Statement:** The data are contained in the article.

**Acknowledgments:** Histology services were provided by the Research Resources Center—Research Histology and Tissue Imaging Core at the University of Illinois at Chicago, established with the support of the Vice Chancellor of Research, Sandra Madueke-Laveaux (University of Chicago), for reviewing the manuscript.



**Conflicts of Interest:** Ayman Al-Hendy is a consultant at Abbvie, Bayer, Allergan, MD Stem Cells for research support. Other authors declare that they have no conflicts of interest.

## Abbreviations

uLMS	Uterine Leiomyosarcoma
LMS	Leiomyosarcoma
LM	Leiomyoma
Ad-Sur-NIS	Adenovirus Survivin-Sodium Iodide Symporter
F18-NaBF <sub>4</sub>	F18-Labeled Sodium Tetrafluoroborate
PET/CT	Positron Emission Tomography/Computed Tomography
FBS	Fetal Bovine Serum
PBS	Phosphate-Buffered Saline
H&E	Hematoxylin and Eosin
SE	Standard Error
SUV	Standardized Uptake Value
ROI	Region of Interest
ALT	Alanine Aminotransferase
ALP	Alkaline Phosphatase
R	Ratio
ULN	Upper Limit of Normal
MRI	Magnetic Resonance Imaging

## References

- Baird, D.D.; Dunson, D.B.; Hill, M.C.; Cousins, D.; Schectman, J.M. High cumulative incidence of uterine leiomyoma in black and white women: Ultrasound evidence. *Am. J. Obstet. Gynecol.* **2003**, *188*, 100–107. [[CrossRef](#)]
- Wise, L.A.; Palmer, J.R.; Stewart, E.A.; Rosenberg, L. Age-specific incidence rates for self-reported uterine leiomyomata in the Black Women’s Health Study. *Obstet. Gynecol.* **2005**, *105*, 563–568. [[CrossRef](#)]
- Laughlin, S.K.; Baird, D.D.; Savitz, D.A.; Herring, A.H.; Hartmann, K.E. Prevalence of uterine leiomyomas in the first trimester of pregnancy: An ultrasound-screening study. *Obstet. Gynecol.* **2009**, *113*, 630–635. [[CrossRef](#)] [[PubMed](#)]
- Sparic, R.; Mirkovic, L.; Malvasi, A.; Tinelli, A. Epidemiology of Uterine Myomas: A Review. *Int. J. Fertil. Steril.* **2016**, *9*, 424–435. [[PubMed](#)]
- Styer, A.K.; Rueda, B.R. The Epidemiology and Genetics of Uterine Leiomyoma. *Best Pract. Res. Clin. Obstet. Gynaecol.* **2015**, *34*, 3–12. [[CrossRef](#)]
- Eltoukhi, H.M.; Modi, M.N.; Weston, M.; Armstrong, A.Y.; Stewart, E.A. The health disparities of uterine fibroid tumors for African American women: A public health issue. *Am. J. Obstet. Gynecol.* **2014**, *210*, 194–199. [[CrossRef](#)] [[PubMed](#)]
- Cui, R.R.; Wright, J.D.; Hou, J.Y. Uterine leiomyosarcoma: A review of recent advances in molecular biology, clinical management and outcome. *Bjog* **2017**, *124*, 1028–1037. [[CrossRef](#)]
- Amant, F.; Coosemans, A.; Debiec-Rychter, M.; Timmerman, D.; Vergote, I. Clinical management of uterine sarcomas. *Lancet Oncol.* **2009**, *10*, 1188–1198. [[CrossRef](#)] [[PubMed](#)]
- D’Angelo, E.; Prat, J. Uterine sarcomas: A review. *Gynecol. Oncol.* **2010**, *116*, 131–139. [[CrossRef](#)]
- Mbatani, N.; Olawaiye, A.B.; Prat, J. Uterine sarcomas. *Int. J. Gynecol. Obstet.* **2018**, *143* (Suppl. 2), 51–58. [[CrossRef](#)]
- Liu, X.; Li, H.; Wu, G.; Cui, S. miR-182 promotes cell proliferation and invasion by inhibiting APC in melanoma. *Int. J. Clin. Exp. Pathol.* **2018**, *11*, 1900–1908. [[PubMed](#)]
- American College of Obstetricians and Gynecologists. Management of Symptomatic Uterine Leiomyomas: ACOG Practice Bulletin, Number 228. *Obstet. Gynecol.* **2021**, *137*, e100–e115. [[CrossRef](#)] [[PubMed](#)]
- American College of Obstetricians and Gynecologists. Uterine Morcellation for Presumed Leiomyomas: ACOG Committee Opinion, Number 822. *Obstet. Gynecol.* **2021**, *137*, e63–e74. [[CrossRef](#)] [[PubMed](#)]
- Bogani, G.; Chiappa, V.; Ditto, A.; Martinelli, F.; Donfrancesco, C.; Indini, A.; Lorusso, D.; Raspagliesi, F. Morcellation of undiagnosed uterine sarcoma: A critical review. *Crit. Rev. Oncol. Hematol.* **2016**, *98*, 302–308. [[CrossRef](#)] [[PubMed](#)]
- Mercorio, A.; Della Corte, L.; Vetrella, M.; Russo, M.; Serafino, P.; Palumbo, M.; Viciglione, F.; Cafasso, V.; Bifulco, G.; Giampaolino, P. Uterine fibroids morcellation: A puzzle topic. *Minim. Invasive Ther. Allied Technol.* **2022**, *31*, 1008–1016. [[CrossRef](#)] [[PubMed](#)]
- Wang, L.; Li, S.; Zhang, Z.; Jia, J.; Shan, B. Prevalence and occult rates of uterine leiomyosarcoma. *Medicine* **2020**, *99*, e21766. [[CrossRef](#)] [[PubMed](#)]
- Bojahr, B.; De Wilde, R.L.; Tchartchian, G. Malignancy rate of 10,731 uteri morcellated during laparoscopic supracervical hysterectomy (LASH). *Arch. Gynecol. Obstet.* **2015**, *292*, 665–672. [[CrossRef](#)]
- Hartmann, K.E.; Fonnesebeck, C.; Surawicz, T.; Krishnaswami, S.; Andrews, J.C.; Wilson, J.E.; Velez-Edwards, D.; Kugley, S.; Sathe, N.A. *Management of Uterine Fibroids*; Agency for Healthcare Research and Quality: Rockville, MD, USA, 2017.

19. Jitsumori, M.; Umeda, A.; Hosoi, A.; Miyanishi, K.; Munakata, S.; Yamamoto, T. Hyperphosphatasemia in leiomyosarcoma of the uterus: Two case reports and a literature review. *J. Obstet. Gynaecol. Res.* **2017**, *43*, 1498–1503. [[CrossRef](#)]
20. Roberts, M.E.; Aynardi, J.T.; Chu, C.S. Uterine leiomyosarcoma: A review of the literature and update on management options. *Gynecol. Oncol.* **2018**, *151*, 562–572. [[CrossRef](#)]
21. Cho, H.; Kim, K.; Kim, Y.; No, J.H. Differential diagnosis between uterine sarcoma and leiomyoma using preoperative clinical characteristics. *J. Obstet. Gynaecol. Res.* **2016**, *42*, 313–318. [[CrossRef](#)]
22. Byar, K.L.; Fredericks, T. Uterine Leiomyosarcoma. *J. Adv. Pract. Oncol.* **2022**, *13*, 70–76.
23. Hata, K.; Hata, T.; Maruyama, R.; Hirai, M. Uterine sarcoma: Can it be differentiated from uterine leiomyoma with Doppler ultrasonography? A preliminary report. *Ultrasound Obstet. Gynecol.* **1997**, *9*, 101–104. [[CrossRef](#)] [[PubMed](#)]
24. Song, K.-J.; Yu, X.-N.; Lv, T.; Chen, Y.-L.; Diao, Y.-C.; Liu, S.-L.; Wang, Y.-K.; Yao, Q. Expression and prognostic value of lactate dehydrogenase-A and -D subunits in human uterine myoma and uterine sarcoma. *Medicine* **2018**, *97*, e0268. [[CrossRef](#)] [[PubMed](#)]
25. Nishigaya, Y.; Kobayashi, Y.; Matsuzawa, Y.; Hasegawa, K.; Fukasawa, I.; Watanabe, Y.; Tokunaga, H.; Yaegashi, N.; Iwashita, M. Diagnostic value of combination serum assay of lactate dehydrogenase, D-dimer, and C-reactive protein for uterine leiomyosarcoma. *J. Obstet. Gynaecol. Res.* **2019**, *45*, 189–194. [[CrossRef](#)]
26. Shalaby, S.; Khater, M.; Laknaur, A.; Arbab, A.; Al-Hendy, A. Molecular Bio-Imaging Probe for Non-Invasive Differentiation Between Human Leiomyoma Versus Leiomyosarcoma. *Reprod. Sci.* **2020**, *27*, 644–654. [[CrossRef](#)] [[PubMed](#)]
27. Huang, R.; Zhao, Z.; Ma, X.; Li, S.; Gong, R.; Kuang, A. Targeting of tumor radioiodine therapy by expression of the sodium iodide symporter under control of the survivin promoter. *Cancer Gene Ther.* **2011**, *18*, 144–152. [[CrossRef](#)] [[PubMed](#)]
28. Spitzweg, C.; O'Connor, M.K.; Bergert, E.R.; Tindall, D.J.; Young, C.Y.; Morris, J.C. Treatment of prostate cancer by radioiodine therapy after tissue-specific expression of the sodium iodide symporter. *Cancer Res.* **2000**, *60*, 6526–6530. [[PubMed](#)]
29. Kim, S.H.; Chung, H.K.; Kang, J.H.; Kim, K.I.; Jeon, Y.H.; Jin, Y.N.; Yun, C.O.; Chung, J.-K.; Kim, E.; Kim, J.-H.; et al. Tumor-targeted radionuclide imaging and therapy based on human sodium iodide symporter gene driven by a modified telomerase reverse transcriptase promoter. *Hum. Gene Ther.* **2008**, *19*, 951–957. [[CrossRef](#)]
30. Scholz, I.V.; Cengic, N.; Baker, C.H.; Harrington, K.J.; Maletz, K.; Bergert, E.R.; Vile, R.; Göke, B.; Morris, J.C.; Spitzweg, C. Radioiodine therapy of colon cancer following tissue-specific sodium iodide symporter gene transfer. *Gene Ther.* **2005**, *12*, 272–280. [[CrossRef](#)]
31. Kakuda, M.; Matsuzaki, S.; Ueda, Y.; Shiomi, M.; Matsuzaki, S.; Kimura, T.; Fujita, M.; Egawa-Takata, T.; Kobayashi, E.; Serada, S.; et al. Copper ions are novel therapeutic agents for uterine leiomyosarcoma. *Am. J. Obstet. Gynecol.* **2020**, *222*, 64.e1–64.e16. [[CrossRef](#)]
32. Skorstad, M.; Kent, A.; Lieng, M. Preoperative evaluation in women with uterine leiomyosarcoma. A nationwide cohort study. *Acta Obstet. Gynecol. Scand.* **2016**, *95*, 1228–1234. [[CrossRef](#)] [[PubMed](#)]
33. Yang, Q.; Ciebiera, M.; Bariani, M.V.; Ali, M.; Elkafas, H.; Boyer, T.G.; Al-Hendy, A. Comprehensive Review of Uterine Fibroids: Developmental Origin, Pathogenesis, and Treatment. *Endocr. Rev.* **2022**, *43*, 678–719. [[CrossRef](#)] [[PubMed](#)]
34. Garcia, N.; Al-Hendy, A.; Barakat, E.C.; Carvalho, K.C.; Yang, Q. Targeting Hedgehog Pathway and DNA Methyltransferases in Uterine Leiomyosarcoma Cells. *Cells* **2020**, *10*, 53. [[CrossRef](#)] [[PubMed](#)]
35. Machado-Lopez, A.; Alonso, R.; Lago, V.; Jimenez-Almazan, J.; Garcia, M.; Monleon, J.; Lopez, S.; Barcelo, F.; Torroba, A.; Ortiz, S.; et al. Integrative Genomic and Transcriptomic Profiling Reveals a Differential Molecular Signature in Uterine Leiomyoma versus Leiomyosarcoma. *Int. J. Mol. Sci.* **2022**, *23*, 2190. [[CrossRef](#)] [[PubMed](#)]
36. Mas, A.; Alonso, R.; Garrido-Gómez, T.; Escorcia, P.; Montero, B.; Jiménez-Almazán, J.; Martín, J.; Pellicer, N.; Monleón, J.; Simón, C. The differential diagnoses of uterine leiomyomas and leiomyosarcomas using DNA and RNA sequencing. *Am. J. Obstet. Gynecol.* **2019**, *221*, 320.e1–320.e23. [[CrossRef](#)]
37. Yang, Q.; Bariani, M.V.; Falahati, A.; Khosh, A.; Lastra, R.R.; Siblino, H.; Boyer, T.G.; Al-Hendy, A. The Functional Role and Regulatory Mechanism of Bromodomain-Containing Protein 9 in Human Uterine Leiomyosarcoma. *Cells* **2022**, *11*, 2160. [[CrossRef](#)]
38. Garcia, N.; Ulin, M.; Ali, M.; Al-Hendy, A.; Carvalho, K.C.; Yang, Q. Evaluation of Hedgehog Pathway Inhibitors as a Therapeutic Option for Uterine Leiomyosarcoma Using the Xenograft Model. *Reprod. Sci.* **2022**, *29*, 781–790. [[CrossRef](#)] [[PubMed](#)]
39. Juang, C.M.; Yen, M.S.; Horng, H.C.; Twu, N.F.; Yu, H.C.; Hsu, W.L. Potential role of preoperative serum CA125 for the differential diagnosis between uterine leiomyoma and uterine leiomyosarcoma. *Eur. J. Gynaecol. Oncol.* **2006**, *27*, 370–374.
40. Zak, K.; Zaremba, B.; Rajtak, A.; Kotarski, J.; Amant, F.; Bobiński, M. Preoperative Differentiation of Uterine Leiomyomas and Leiomyosarcomas: Current Possibilities and Future Directions. *Cancers* **2022**, *14*, 1966. [[CrossRef](#)]
41. Xie, H.; Zhang, X.; Ma, S.; Liu, Y.; Wang, X. Preoperative Differentiation of Uterine Sarcoma from Leiomyoma: Comparison of Three Models Based on Different Segmentation Volumes Using Radiomics. *Mol. Imaging Biol.* **2019**, *21*, 1157–1164. [[CrossRef](#)]
42. Hélage, S.; Vandeventer, S.; Buy, J.-N.; Bordonné, C.; Just, P.-A.; Jacob, D.; Ghossain, M.; Rousset, P.; Dion, É. Uterine Sarcomas: Are There MRI Signs Predictive of Histopathological Diagnosis? A 50-Patient Case Series with Pathological Correlation. *Sarcoma* **2021**, *2021*, 8880080. [[CrossRef](#)] [[PubMed](#)]
43. Chiappa, V.; Interlenghi, M.; Salvatore, C.; Bertolina, F.; Bogani, G.; Ditto, A.; Martinelli, F.; Castiglioni, I.; Raspagliesi, F. Using rADioMIcs and machine learning with ultrasonography for the differential diagnosis of myometrial tumors (the ADMIRAL pilot study). Radiomics and differential diagnosis of myometrial tumors. *Gynecol. Oncol.* **2021**, *161*, 838–844. [[CrossRef](#)] [[PubMed](#)]

44. Della Badia, C.; Karini, H. Endometrial stromal sarcoma diagnosed after uterine morcellation in laparoscopic supracervical hysterectomy. *J. Minim. Invasive Gynecol.* **2010**, *17*, 791–793. [[CrossRef](#)] [[PubMed](#)]
45. Rodriguez, A.M.; Asoglu, M.R.; Sak, M.E.; Tan, A.; Borahay, M.A.; Kilic, G.S. Incidence of occult leiomyosarcoma in presumed morcellation cases: A database study. *Eur. J. Obstet. Gynecol. Reprod. Biol.* **2016**, *197*, 31–35. [[CrossRef](#)] [[PubMed](#)]
46. Sharma, R.; Aboagye, E. Development of radiotracers for oncology—The interface with pharmacology. *Br. J. Pharmacol.* **2011**, *163*, 1565–1585. [[CrossRef](#)]
47. Jiang, H.; DeGrado, T.R. [<sup>18</sup>F]Tetrafluoroborate ([<sup>18</sup>F]TFB) and its analogs for PET imaging of the sodium/iodide symporter. *Theranostics* **2018**, *8*, 3918–3931. [[CrossRef](#)]
48. Vallabhajosula, S. <sup>18</sup>F-labeled positron emission tomographic radiopharmaceuticals in oncology: An overview of radiochemistry and mechanisms of tumor localization. *Semin. Nucl. Med.* **2007**, *37*, 400–419. [[CrossRef](#)]
49. O’doherly, J.; Jauregui-Osoro, M.; Brothwood, T.; Szyszko, T.; Marsden, P.K.; O’doherly, M.J.; Cook, G.J.; Blower, P.J.; Lewington, V. <sup>18</sup>F-Tetrafluoroborate, a PET Probe for Imaging Sodium/Iodide Symporter Expression: Whole-Body Biodistribution, Safety, and Radiation Dosimetry in Thyroid Cancer Patients. *J. Nucl. Med.* **2017**, *58*, 1666–1671. [[CrossRef](#)]

**Disclaimer/Publisher’s Note:** The statements, opinions and data contained in all publications are solely those of the individual author(s) and contributor(s) and not of MDPI and/or the editor(s). MDPI and/or the editor(s) disclaim responsibility for any injury to people or property resulting from any ideas, methods, instructions or products referred to in the content.